Inversion of Bubble Size Distribution Based on Whale Optimization Algorithm

Zhenzhong Lu, Ziqi Hu, Lin Ma, Shangtao Huang, Tao Peng, Min Liu, Biao Han, Jiali Liao, Zihao Wang, and Yanling Sun

***Abstract*—A particle size inversion method based on whale optimization algorithm (WOA) is presented. In the experiment, the small angle forward scattering measurement system is used to conduct experimental research on the inversion of bubble particle size. WOA is used to invert and simulate the bubbles that follow a certain distribution, adding different levels of random noise to verify the stability of the algorithm. The results verify the feasibility and stability of applying WOA to particle size inversion.**

***Index Terms*—Whale optimization algorithm, small angle forward scattering method, bubble size distribution.**

I. Introduction

PARTICLES refer to tiny solid, liquid or gas in condition of segmentation, which is either dispersed in a liquid medium or dispersed in a gaseous medium to form a two-phase substance. The accurate detection of particle size characteristics and their distribution is of great significance for many fields, such as chemical production [1], material preparation [2], medicinal products [3], environment monitoring [4] and so on. There are many methods for particle size measurement. The image method is the most direct but the accuracy is limited, while the ultrasonic method will destroy the particles and lead to errors in the results [5]. The optical measurement technology based on the principle of light scattering has been widely studied and applied in recent years, with the advantages of non-contact, real-time and rapid, wide particle size measurement range, wide applicability and high measurement accuracy [6], [7], [8], [9], [10]. The solution of particle size distribution is essentially to solve the first Fredholm integral problem [6]. This kind of problem is difficult to solve stably because of its inadequacy, so the non-independent mode algorithm is usually used in the light scattering measurement.

Traditional optimization algorithms such as Levenberg-Marquardt (L-M) method, simplex method and quasi-Newton method have the disadvantages of slow speed and easy to fall into local optimality. In recent years, many researchers have tried to apply some intelligent optimization algorithms with better global performance to particle size inversion. The common non-independent model intelligent optimization algorithms, such as the genetic algorithm, the cuckoo algorithm, the artificial fish swarm algorithm and the artificial bee colony algorithm are easy to fall into local optimal solutions, and have poor performance when facing high-dimensional complex problems and engineering design [11], [12], [13], [14]. As a swarm intelligence optimization algorithm, the whale optimization algorithm (WOA) has the advantages of easy to jump out of the local optimal solution, good globality, and fast solution speed [15].

We choose the WOA to invert the bubble size, and the bubble size distribution inversion algorithm is analyzed and simulated theoretically as well as the robustness of the WOA is detected by adding noise. Experimentally, a small angle forward scattering wake bubble size measurement experimental device is used to carry out multiple sets of experimental measurements to verify the particle size distribution of the WOA inversion. Basing on the WOA inversion, the particle size distribution is basically consistent with the actual particle size distribution, which shows that this method has certain feasibility in solving the problem of particle size inversion distribution, and can be used in the research field that needs to measure the particle size distribution.

II. Inversion Algorithm and Simulation of Particle Size Distribution

A. Bubble Particle Size Inversion Algorithm

Assuming that the particle size of the bubble group to be measured follows the probability distribution $N(D)$ and the scattered light intensity of each bubble is $I_{\mathrm{Mie}}(\theta, D, m)$, the total scattered light intensity received $I_s(\theta)$ is expressed as follows:

$$I_s(\theta) = \int_{D_{\min}}^{D_{\max}} I_{\mathrm{Mie}}(\theta, D, m)\, N(D)\, \mathrm{d}D, \tag{1}$$

where $D_{\max}$ and $D_{\min}$ respectively represent the diameters of the largest and smallest bubbles. Equation (1) is the first Fredholm integral equation, which can be simplified as follows:

$$I_s(\theta_i) = \sum_j I_{\mathrm{Mie}}(\theta_i, D_j, m)\, N(D_j), \tag{2}$$

Manuscript received 9 March 2024; revised 21 May 2024; accepted 26 May 2024. Date of publication 30 May 2024; date of current version 11 June 2024. *(Corresponding author: Lin Ma.)*

The authors are with the School of Optoeletronic Engineering, Xidian University, Xi'an 710071, China (e-mail: 22191215013@stu.xidian.edu.cn).

Digital Object Identifier 10.1109/JPHOT.2024.3406886

which can be expanded as Eq. (3):

$$\mathbf{I_s} = \begin{bmatrix} I_{\mathrm{s}}(\theta_1) \\ I_{\mathrm{s}}(\theta_2) \\ \vdots \\ I_{\mathrm{s}}(\theta_i) \end{bmatrix} = \begin{bmatrix} I_{\mathrm{Mie}}(\theta_1, D_1, m), I_{\mathrm{Mie}}(\theta_1, D_2, m), \ldots, I_{\mathrm{Mie}}(\theta_1, D_j, m) \\ I_{\mathrm{Mie}}(\theta_2, D_1, m), I_{\mathrm{Mie}}(\theta_2, D_2, m), \ldots, I_{\mathrm{Mie}}(\theta_2, D_j, m) \\ \vdots \\ I_{\mathrm{Mie}}(\theta_i, D_1, m), I_{\mathrm{Mie}}(\theta_i, D_2, m), \ldots, I_{\mathrm{Mie}}(\theta_i, D_j, m) \end{bmatrix} \cdot \begin{bmatrix} N(D_1) \\ N(D_2) \\ \vdots \\ N(D_j) \end{bmatrix} = \mathbf{A} \cdot \mathbf{N}. \tag{3}$$

Where, $\mathbf{I_s}$ is the column vector of real measured light intensity distribution, and $I_s(\theta_i)$ represents the light intensity received by the *i*th pixel on the linear array CCD. **A** is the intensity coefficient matrix of magnitude $i \times j$. $A_{i,j} = I_{\mathrm{Mie}}(\theta_i, D_j, m)$ is the theoretical value of light intensity scattered by the bubble with particle size D_j on the *i*th pixel, θ_i is the scattering angle corresponding to the *i*th pixel, and *m* is the relative refractive index. **N** is the column vector of particle size distribution, and $N(D_j)$ represents the number probability of bubbles with particle size D_j in the area to be measured. Therefore, the inversion of particle size distribution $N(D)$ can be realized by solving Eq. (3).

B. Bubble Size Inversion in Constrained Mode Base on WOA

The WOA is to compare the optimization process of the algorithm to the process of whales searching for prey, uses simulations to break down the whale's predatory behavior into three actions: encircling prey, bubble net attack, and search for prey [15]. We can see the basic calculation flow of WOA in Fig. 1, and then we also show and analyze the formulas of the three stages of WOA.

1) Encircling Prey: The position of the leading whale as the optimal search individual is denoted as X_P, and the position of other whale is denoted by *X*.

$$\overrightarrow{d} = \left| \overrightarrow{C} \cdot \overrightarrow{X_P}(k) - \overrightarrow{X}(k) \right|, \tag{4}$$

$$\overrightarrow{X}(k+1) = \overrightarrow{X_P}(k) - \overrightarrow{H} \cdot \overrightarrow{d}. \tag{5}$$

Where *d* is the absolute value of the distance between the whale and the prey, $k \in [1, k_{\max}]$ is the number of iterations, and the vectors *H* and *C* can refer to [15].

2) Bubble Net Attack: The spiral motion equation of a whale in a bubble net attack is as follows:

$$\vec{d}' = \left| \overrightarrow{X_P}(k) - \overrightarrow{X}(k) \right|, \tag{6}$$

$$\overrightarrow{X}(k+1) = \vec{d}' \cdot e^{bl} \cdot \cos(2\pi l) + \overrightarrow{X_P}(k), \tag{7}$$

Where, *b* can determine the trajectory of the whale's spiral movement, usually 1, $l \in [-1, 1]$ is a random number. When *p* < 0.5, encircling the prey, and $p \geq 0.5$, hunting the prey.

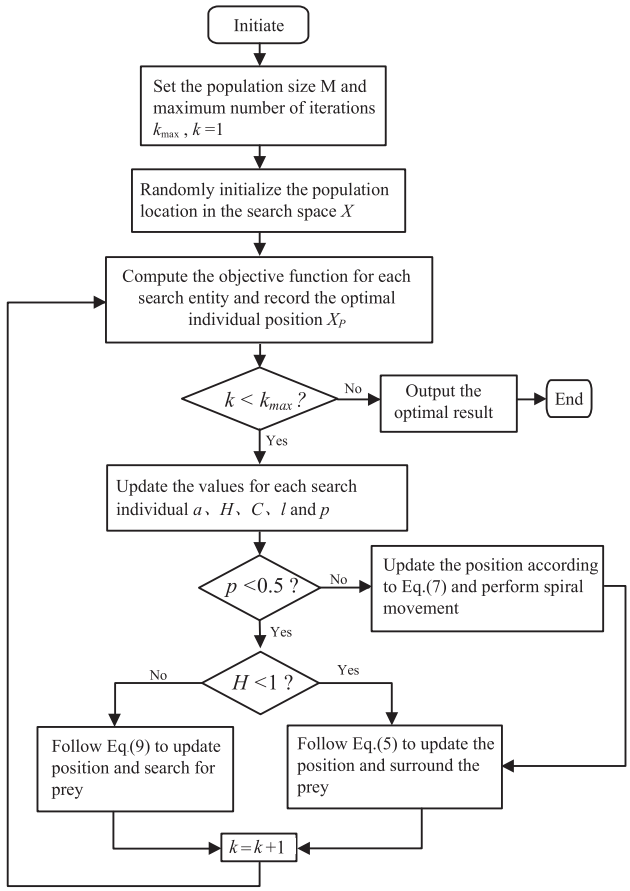

Fig. 1. Flowchart of whale optimization algorithm.

$$X(k+1) = \begin{cases} X_P(k) - H \cdot d & \text{if } p < 0.5, \\ d' \cdot e^{bl} \cdot \cos(2\pi l) + X_P(k) & \text{if } p \geq 0.5. \end{cases} \tag{8}$$

3) Search for Prey: As described in [15]: when $H \geq 1$, the position of an individual whale is randomly selected in the individual population as a reference, and the position update formula is as follows:

$$\overrightarrow{X}(k+1) = \overrightarrow{X_r}(k) - \overrightarrow{H} \cdot \vec{d}'', \tag{9}$$

$$\vec{d}'' = \left| \overrightarrow{C} \cdot \overrightarrow{X_r}(k) - \overrightarrow{X}(k) \right|. \tag{10}$$

Where X_r is the position of the randomly selected individual whale, and d'' is the absolute value of the distance.

In order to verify the feasibility of the WOA. Here, we use this algorithm to invert the bubble particle size. Assuming that the characteristic particle size parameter $\bar{D}$ of the original particle size distribution of the bubble is 70 μm, and the particle size distribution width parameter σ is 5, the original particle size distribution of the bubble is shown in Fig. 2. In addition, 3%, 5% and 10% random noises are added to the simulation calculation to verify the anti-noise performance of the algorithm. The parameters of scattering light intensity matrix **A** are as follows:

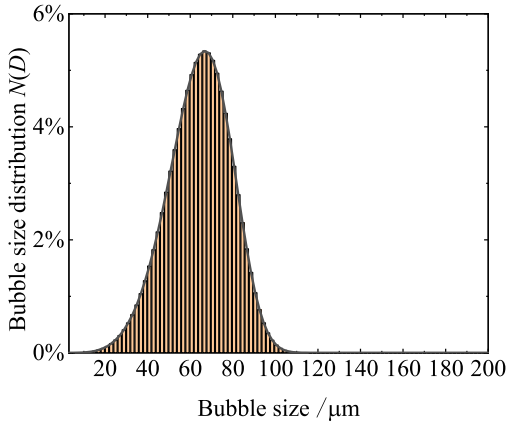

Fig. 2. Original distribution of bubble size.

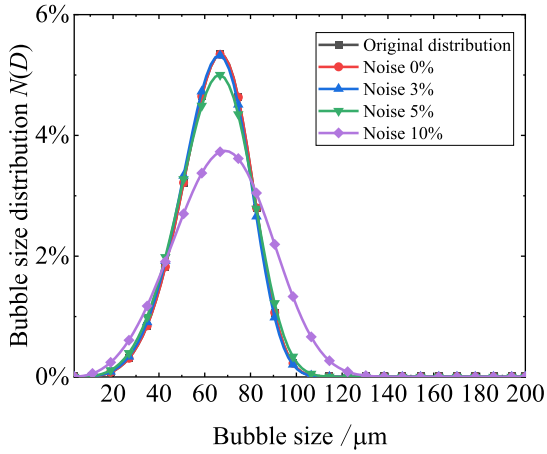

Fig. 3. Bubble size distribution of WOA inversion under different noise levels.

TABLE I
PARAMETER SETTING OF WOA

Size M	Dimension of problem	Iterations $k_{\max}$	Search space
200	2	50	$\bar{D}\in[3,200]$ $\sigma\in[0,40]$

TABLE II
INVERSION RESULTS OF WOA

Noise	Average value $(\bar{D},\sigma)$	Standard deviation $(\bar{D},\sigma)$
0%	(69.999,5.006)	(0.049,0.038)
3%	(69.757,4.915)	(0.029,0.025)
5%	(69.947,4.674)	(0.026,0.020)
10%	(75.046,3.685)	(0.011,0.009)

the wavelength of the incident light is 532 nm, the receiving angle of the scattering light intensity ranges from 0 to 6.657°, the dispersion is 149 points, the particle size ranges from 3 to 200 μm, and the particle size intervals are divided into 100 at equal intervals, then the coefficient matrix **A** is a matrix of order. The parameter settings for WOA are shown in Table I.

We use WOA to solve the objective function under these three types of noise for 20 times respectively. The average value and standard deviation of the 20 groups of solutions are obtained, as shown in Table II. The bubble particle size distribution curve drawn according to the average values of $\bar{D}$ and σ in the table is shown in Fig. 3.

By analyzing the above information, we can find that: when the noise level is below 10%, the mean value of $\bar{D}$ obtained by inversion is very close to 70 μm, while when the noise level is 10%, the obtained $\bar{D}$ is 75.046 μm, and the relative error is 7.21%. The parameter σ decreases with the increase of noise, indicating that noise will widen the particle size distribution curve and the

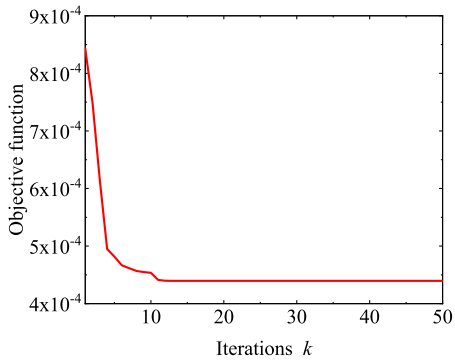

Fig. 4. The iterative process of the WOA.

larger the noise, the wider the width. From Table II, it can be seen that the results obtained by running 20 times under different noise levels have little difference, which indicates the stability of the algorithm. When the noise level is low, the obtained results are basically consistent with the original distribution. When the noise level is 5%, the peak value of the particle size distribution decreases and the curve widens compared with the original distribution. When the noise is 10%, not only is the peak significantly reduced, the particle size corresponding to the peak is increased, but the curve broadening is also very obvious.

Here, we record the variation of the objective function with k during the WOA operation when the noise level is 3%, as shown in Fig. 4. We can see that the WOA converges quickly in the iterative process, and the value of the objective function can converge to a small value in the 10th iteration, and the calculation efficiency is high. The data analysis shows that the WOA used in the measurement of bubble size distribution has certain accuracy and reliability.

C. Bubble Size Inversion Simulation Based on Chahine

The Chahine algorithm originally been used to measure atmospheric temperature distribution, and further research found that it can also be applied to particle measurement. The iterative

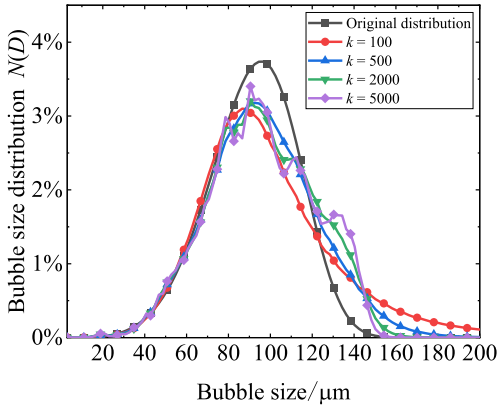

Fig. 5. Iterative results of Chahine algorithm under noises.

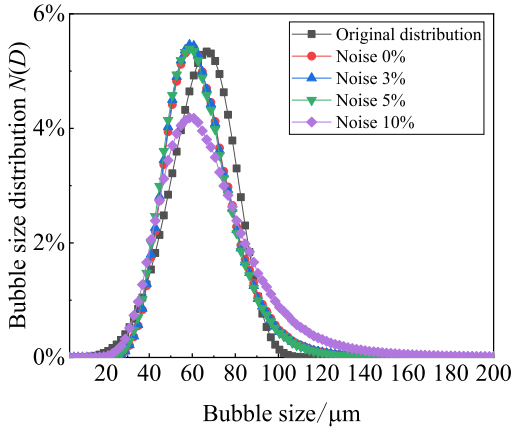

Fig. 6. When $k = 40000$, the bubble size distribution of Chahine algorithm under different noise levels.

formula of Chahine algorithm is shown as (11):

$$\begin{cases} \mathbf{I}_{\mathbf{s}}^{(k)} = \mathbf{A}\mathbf{N}^{(k)} \\ h^{(k)} = \mathbf{I}_{\mathbf{s}} ./ \mathbf{I}_{\mathbf{s}}^{(k)} \\ c^{(k)} = \left(\mathbf{A}^T h^{(k)}\right) ./ \mathrm{sum}\left(\mathbf{A}^T\right) \\ \mathbf{N}^{(k+1)} = c^{(k)} .* \mathbf{N}^{(k)} \end{cases} \tag{11}$$

Where k represents the number of iterations, and "sum" is the operator for summing matrix columns. The outstanding advantages of the Chahine algorithm are fast convergence speed, simple iteration formula, good results can be obtained without noise interference, and the initial value of the particle size distribution column vector has little influence on the iterative results. However, the disadvantages of this algorithm are also obvious. As shown in Fig. 5. when the measured data contains noise, the results obtained will not get better with the increase of the number of iterations, and the optimal number of iterations will change with the difference of the noise level [16]. Because the rising movement of the bubble causes the distribution of scattered light to change to some extent, so that the noise level is different at different times, it is difficult to select the number of iterations when using this algorithm to measure the bubbles.

In order to conduct a comparative study with WOA, we select the Chahine algorithm to invert bubbles at different noise levels, and the bubble size curve distribution is shown in Fig. 6. It can be seen that the inversion results obtained by the Chahine algorithm are somewhat deviated from the original bubble size distribution. When the noise level increases, the peak value of the bubble size distribution curve decreases and widens. By comparing the results obtained from the WOA inversion in Fig. 3, it can be found that the WOA results are better than the Chahine results at the same noise level.

III. Experiment

A. Experimental System Introduction

The process of the experiment is as follows: firstly, the extended collimated beam is irradiating onto a group of bubbles in a cylinder. The incident light is scattered by a group of bubbles and received by a fourier lens, forming a circularly symmetric scattered light field on the rear focal plane of the lens. The scattering light intensity data is collected by linear array CCD and transmitted to the computer for storage and analysis. The experimental system is shown in Fig. 7. The model and parameters of the experimental device are shown in Table III.

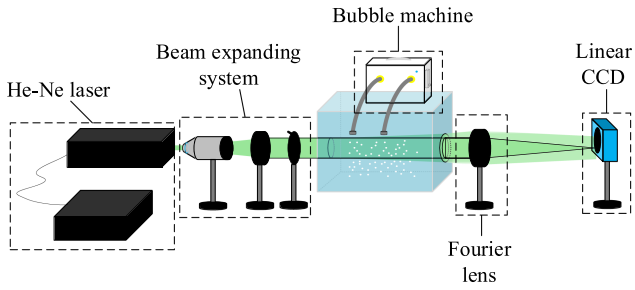

Fig. 7. Small angle forward scattering wake bubble particle size measurement system.

TABLE III
THE MODEL AND PARAMETERS OF THE EXPERIMENTAL DEVICE

He-Ne laser	Type: LSR-PS-FA, λ: 532nm, Δυ <0.1nm, θ = 2mrad
Beam expanding system	Microscope(×40), Lens (f=115mm), Diaphragm
Fourier lens	f=300mm
Linear CCD	pixels number: 7450; pixel size:4.7μm×4.7μm

B Inversion of Bubble Size Distribution

1) Tracer Particle Inversion: Tracer particles of different sizes are dropped to verify the effectiveness of the experimental

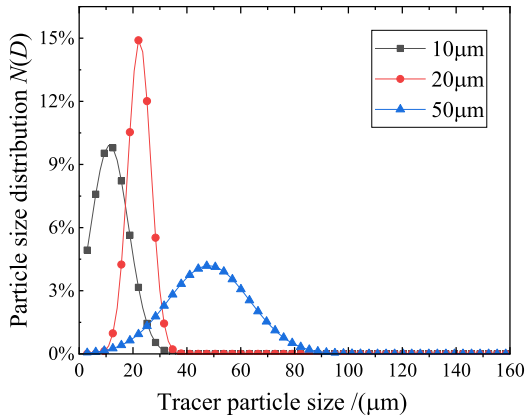

Fig. 8. The solution results of tracer particle size distribution.

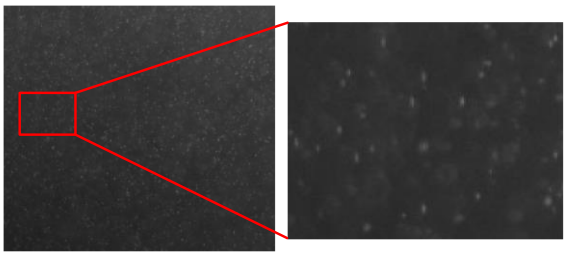

Fig. 9. Bubbles image taken by camera.

Fig. 10. Comparison of forward scattered light before and after bubble formation:(a) pre-bubble and (b) post-bubble.

system. Here, we use the WOA to solve the scattered light intensity distribution of these three particles, and obtain the tracer particle size distribution as shown in Fig. 8. We can see that the peak values of particle size distribution curves obtained by WOA are about 10 μm, 20 μm, and 50 μm, respectively. And these three tracer size distribution curves have a certain broadening, indicating that there is a certain range of particle size. It may also because the impurities in the water and the impurities in the air will also have a certain scattering of the laser, which will affect the experimental results.

2) Measurement of Bubble Size Distribution: Firstly, estimating the bubble size range use image method. Here, we get bubble size d in the figure is between 5.3∼26.5 μm. Then, by incorporating the image method formula, we can obtain the actual size D of the bubble can be obtained between 27.56∼137.8 μm. The following Fig. 9. is an image of bubbles.

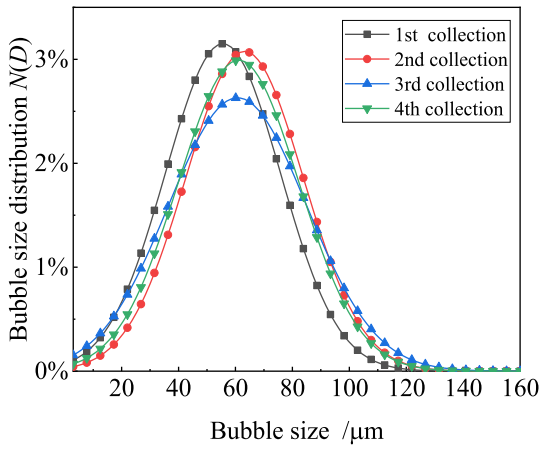

Fig. 11. Particle size distribution of bubbles obtained under different collection times.

Fig. 10. is a comparison of the scattered light before and after the bubble is generated in the experiment. It can be seen that after the laser is scattered by the bubble and deviates from the original propagation direction, thus enlarging the light spot at the focal plane of the lens.

Fig. 11. shows the bubble size distribution obtained using WOA at different collection times. It can be seen that: the particle size of the bubbles is mainly concentrated in the range of 20∼140 μm, which is consistent with the results of the image method. The peak value of the particle size distribution curve is about 60 μm, indicating that the bubbles with a size of about 60 μm are the most. Comparing the four curves in the Fig. 11, we can see that the particle size distribution of the bubbles collected four times changes very little.

IV. Conclusion

A constraint-mode particle size inversion simulation method based on whale optimization algorithm is presented. The stability of the algorithm is verified by adding noise during the simulation. The bubble particle size measurement system is used to measure the bubble particle size mainly in the range of 20∼140 μm, and the bubble particle size range obtained by WOA inversion is basically consistent with the experimental measurement. The validity, feasibility and stability of measuring the particle size distribution of bubble wake based on light scattering method and whale optimization algorithm are verified.

References

[1] S. Sampa and S. C. Joachim, "Recent developments in multilayered polymeric particles–from fabrication techniques to therapeutic formulations," *J. Mater. Chem. B*, vol. 3, no. 17, pp. 3406–3419, Apr. 2015, doi: 10.1039/C5TB00086F.

[2] D. Y. Liu, C. O'Sullivan, and J. A. H. Carraro, "The influence of particle size distribution on the stress distribution in granular materials," *Géotechnique*, vol. 73, no. 3, pp. 250–264, Mar. 2023, doi: 10.1680/jgeot.21.00127.

[3] F. Caputo, J. Clogston, L. Calzolai, M. Rosslein, and A. Prina-Mello, "Measuring particle size distribution of nanoparticle enabled medicinal products, the joint view of EUNCL and NCI-NCL. A step by step approach combining orthogonal measurem-ents with increasing complexity," *J. Controlled Release*, vol. 299, pp. 31–43, Apr. 2019, doi: 10.1016/j.jconrel.2019.02.030.

[4] D. Koestner, D. Stramski, and R. A. Reynolds, "Characterization of suspended particulate matter in contrasting coastal marine environments with angle-resolved polarized light scattering measurements," *Appl. Opt.*, vol. 60, no. 36, pp. 11161–11179, Nov. 2021, doi: 10.1364/AO.441226.

[5] M. Uher and P. Benes, "Measurement of particle size distribution by the use of acoustic emission method," in *Proc. IEEE Int. Instrum. Meas. Technol. Conf.*, 2012, pp. 1194–1198.

[6] S. Y. Cai, J. D. Mao, H. Zhao, C. Y. Zhou, X. Gong, and H. J. Sheng, "Inversion algorithm for non-spherical dust particle size Distributions," *Opt. Rev.*, vol. 26, no. 3, pp. 319–331, Jun. 2019, doi: 10.1007/s10043-019-00505-7.

[7] B. R. Angara, P. Shanmugam, and H. Ramachandran, "Inversion of volume scattering function for estimation of bubble size distribution in ocean waters," *IEEE Access*, vol. 9, pp. 135069–135078, Oct. 2021, doi: 10.1109/ACCESS.2021.3115253.

[8] G. Q. Huang et al., "Effect of directional movement on dynamic light scattering," *IEEE Photon. J.*, vol. 13, no. 3, Jun. 2021, Art. no. 5000213, doi: 10.1109/JPHOT.2021.3083611.

[9] X. H. He, Q. G. Zhang, R. Zhang, C. Guo, and X. W. Wu, "Research on detection technology of bubble size distribution in transformer oil based on MIE scattering theory," in *Proc. 22nd Int. Symp. High Voltage Eng.*, 2021, pp. 1740–1743.

[10] Q. Ma, H. Y. Zuo, H. P. Xia, P. P. Liu, and G. D. Zhang, "Influence of dispersion on particle size-distribution based on multi-wavelength scattering measurement," *Opt. Eng.*, vol. 60, no. 3, Mar. 2021, Art. no. 034111, doi: 10.1117/1.OE.60.3.034111.

[11] J. Dai and J. Q. Shen, "Application of genetic algorithm in particle size measurement technology based on forward light scattering," *Acta Photonica Sinica*, vol. 50, no. 5, pp. 0512002, Jun. 2021, doi: 10.3788/gzxb20215005.0512002.

[12] H. H. Zhan, T. T. Zha, B. Hong, and L. Shan, "Particle size distribution inversion using the Weibull-distribution adaptive-parameters cuckoo search algorithm," *Appl. Opt.*, vol. 62, no. 1, pp. 235–245, 2023, doi: 10.1364/AO.476741.

[13] P. Farhad, R. Wang, C. P. Lim, X. Z. Wang, and D. Yazdani, "A review of artificial fish swarm algorithms: Recent advances and applications," *Artif. Intell. Rev.*, vol. 56, no. 3, pp. 1867–1903, Mar. 2023, doi: 10.1007/s10462-022-10214-4.

[14] L. Shan, H. R. Li, B. Hong, D. D. Wang, T. T. Zha, and M. Kong, "Inversion of multimodal particle size distribution based on the artificial bee colony algorithm," *Acta Photonica Sinica*, vol. 49, no. 12, Dec. 2020, Art. no. 1229002, doi: 10.3788/gzxb20204912.1229002.

[15] X. L. Wang, L. Y. Zhang, J. H. Chai, and T. Fei, "A summary of the research on whale optimization algorithms," in *Proc. Int. Conf. Algorithms, Microchips, Netw. Appl.*, 2022, pp. 121760U–1–121760U–4.

[16] L. X. Cao, J. Zhao, M. Kong, L. Shan, and T. T. Guo, "Inversion of particle size distribution based on improved Chahine algorithm," *Infrared Laser Eng.*, vol. 44, no. 9, pp. 2837–2843, Sep. 2015, doi: 10.3969/j.jssn.1007-2276.2015.09.051.